

The Early Cretaceous Absolute Geomagnetic Paleointensity Based on Results for Traps of the Franz Josef Land Archipelago

V. V. Abashev^{a,b,*}, Corresponding Member of the RAS D. V. Metelkin^{a,b}, A. A. Eliseev^{a,b},
Academician V. A. Vernikovskiy^{a,b}, N. E. Mikhaltsov^{a,b}, and E. V. Vinogradov^{a,b}

Received May 21, 2024; revised July 8, 2024; accepted July 9, 2024

Abstract—Data on the absolute value of the geomagnetic field intensity at the beginning of the Cretaceous Normal Superchron (C34n) was obtained from basalts of Hooker Island of the Franz Josef Land archipelago (FJL). These basalts are considered as one of the manifestations of the High Arctic Large Igneous Province. The record of the ancient geomagnetic field in the studied Early Cretaceous basalts was preserved well due to the presence of pseudo-single domain grains of primary magmatic titanomagnetite. The paleointensity, obtained by the Thellier–Coe method, satisfies the generally accepted reliability criteria, taking into consideration other necessary evidence. This information indicates that 125 Ma, during the formation of the FJL traps, the intensity of the geomagnetic field was four times lower than today. Our estimates show that the mean value of the virtual dipole moment was 1.7×10^{22} Am². These results support the views about the low paleointensity at the Barremian–Aptian boundary and indicate a correlation between the intensity of the geomagnetic field, the frequency of reversals, and the formation of mantle plumes.

Keywords: paleomagnetism, paleointensity, Cretaceous superchron C34n, Thellier–Coe method, traps, Franz Josef Land archipelago, large igneous provinces

DOI: 10.1134/S1028334X2460275X

Throughout geological history, the magnetic field has been affected by multiple reversals. According to the Geomagnetic Polarity Time Scale (GPTS), over the past 170 Myr, most magnetochrons have lasted from 0.1 to 1 Myr. The only exception is the long Cretaceous, Aptian to Santonian (121–84 Ma) superchron (designated CNS, Jalal or C34n), when for ~40 Myr, the Earth's magnetic field was characterized by normal polarity, with an almost complete absence of reversals. According to theoretical models [1–4], such a long time interval of the stable state of the geomagnetic field reflects the restructuring of deep thermodynamic processes, including those in the outer liquid core. These processes are caused by the removal of accumulated excess heat by plumes arising at the core–mantle boundary and/or by the activation of convective currents in the mantle. Accordingly, the intervals of the superchrons should be characterized by a prevailing high intensity of the geomagnetic field. This is generally confirmed by results of statistical analysis of the paleointensity database, which indicate

the existence of an inverse correlation between the frequency of reversals and the intensity of the geomagnetic field [5]. Thus, most of the determinations available for the C34n interval correspond to average values of the virtual dipole moment (VDM) of 4.8×10^{22} Am². In this case, the beginning of the epoch of a relatively high geomagnetic field, according to the results of this analysis, is scheduled shortly before the beginning of the superchron, about 135 Ma. The Jurassic–Early Cretaceous (200–135 Ma) interval preceding it is characterized by frequent reversals; the VDM values corresponding to this interval are comparatively lower, on average, 2.5×10^{22} Am². However, a number of studies [6, 7] present the actual data rejecting such a correlation of VDM with the frequency of reversals and testifying to the presence of intervals of the extremely weak geomagnetic field during C34n. Within the framework of this problem, it is necessary to accumulate sound data on the paleointensity for the Jurassic–Cretaceous interval. The most suitable source of such data is volcanic sections of large igneous provinces. The basaltic sheets of the FJL, which represent one of the areas of the Barents Sea part of the High Arctic Large Igneous Province (HALIP), became the direct object of our study. Until the present, the FJL basalts have been studied in detail with respect to the preservation and orientation of the vector of natural remanent magnetization [8, 9]. Using

^aTrofimuk Institute of Petroleum Geology and Geophysics, Siberian Branch, Russian Academy of Science, Novosibirsk, 630090 Russia

^bNovosibirsk State University, Novosibirsk, 630090 Russia

*e-mail: abashev@ipgg.sbras.ru

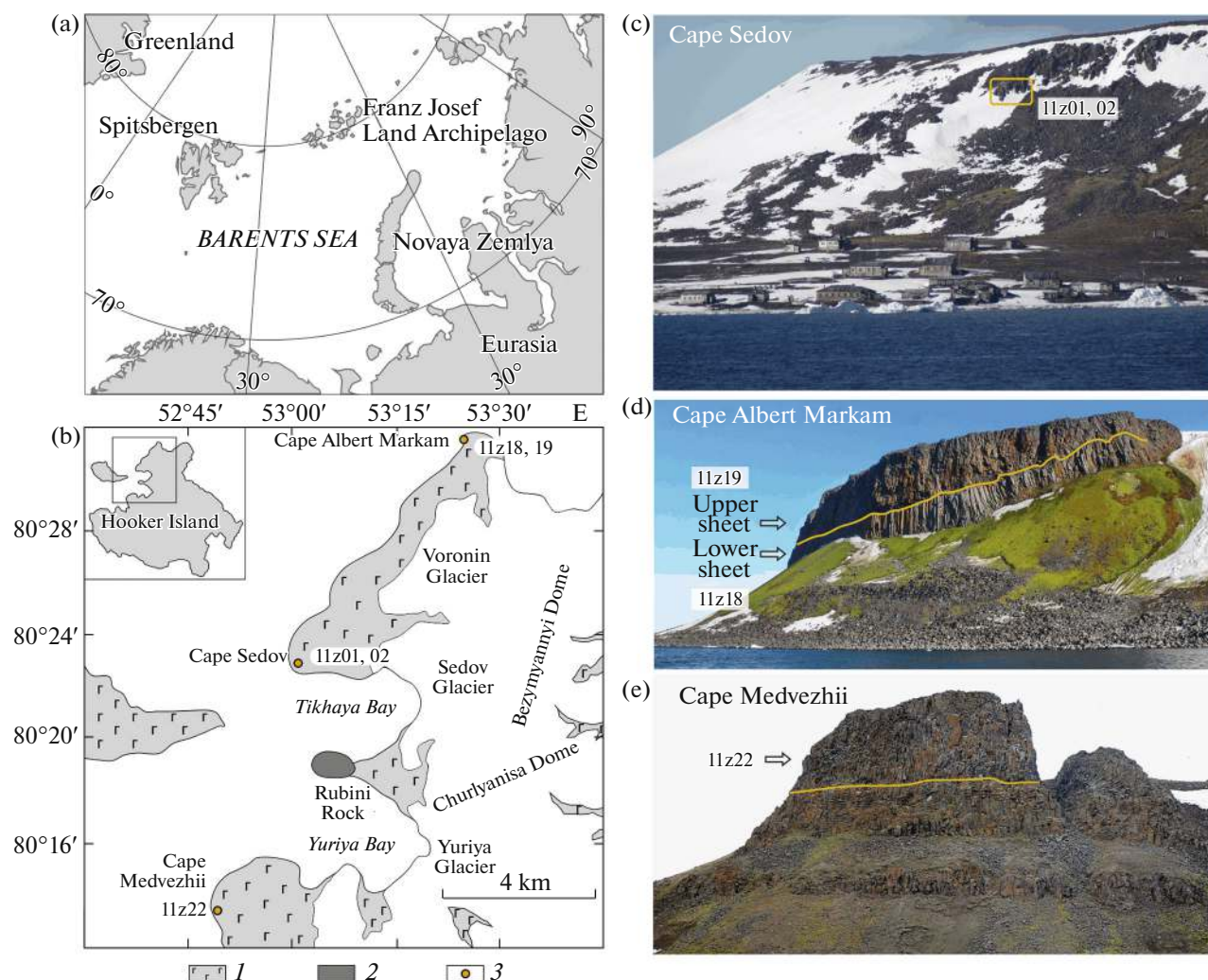


Fig. 1. Geology of the northern part of Hooker Island, Tikhaya Bay area. (a) Scheme of the location of the Franz Josef Land archipelago; (b) geology of Hooker Island. (1) Early Cretaceous basalts and dolerites undifferentiated; (2) Rubini Rock stock; (3) paleomagnetic sampling points; (c) general view of the Tikhaya Bay cliff with the location of outcrop 11z01, 02; (d) photo of the section at Cape Albert Markam with the location of outcrop 11z18, 19; (e) photo of the section at Cape Medvezhii with the location of outcrop 11z22.

geochronological data, it has been proved that the formation of the basalts and the record of the paleomagnetic signal established in them occurred at the end of the Barremian–Aptian time (125 Ma).

Here we present the first for the FJL results of the study of paleointensity on the example of a series of thick basalt sheets armoring Hooker Island. In particular, the basalts presented in this analysis were sampled in Tikhaya Bay east of Cape Sedov and in outcrops at Cape Albert Markam and Cape Medvezhii (Fig. 1).

The carrier of primary magnetization in the studied basalts is titanomagnetite with Curie temperatures of ~250–300°C [8, 9]. In the same range, the main part of the natural remanence is lost during the stepwise thermal demagnetization. At heating not higher than 300°C, significant mineralogical changes in the sam-

ples almost do not occur. Analysis of the hysteresis parameters indicates the predominance of pseudo-single-domain, less often even smaller single-domain particles [8, 9]. In general, the petromagnetic characteristics, magnetic mineralogy, and the results of the study of the component composition of remanence indicate the potential prospects for determining the absolute paleointensity of the Earth magnetic field.

The absolute paleointensity values B_{anc} were determined using the Thellier–Coe method with the partial thermoremanent magnetizations pTRM-check procedure [10]. The Arai–Nagata (AN) and Zijderveld diagrams have common features for most of the samples studied (Fig. 2). Primarily, two components are traced on them. At the first steps of demagnetization, already at 100–120°C, the chaotically oriented component, which has a viscous nature, is

Table 1. B_{anc} mean values by the Thellier–Coe method and the corresponding VDM

Sampling site	Paleointensity					VDM $\times 10^{22} \text{ Am}^2$		
	N/n	$B_{anc}, \mu\text{T}$	$B_{anc},$ St.err μT	$B_{anc},$ St.err %	$B_{anc},$ St.dev. μT	VDM	VDM, St.err	VDM, St.dev
11z01, 02	12/12	11.3	0.6	5.4	2.1	1.6	0.1	0.3
11z18	8/8	12.3	0.8	6.7	2.3	1.7	0.1	0.3
11z19	8/8	12.2	1.1	8.7	3.0	1.7	0.2	0.4
11z22	10/10	13.2	0.7	5.5	2.3	1.9	0.1	0.3

N/n is the number used in statistics to the total number of studied samples; St.err is standard error; St.dev is standard deviation.

destroyed. Predominantly upon heating from $\sim 160^\circ\text{C}$ and up to the complete loss of natural remanence, the only regular characteristic component is isolated. In the AN-diagrams, the pTRM-checks coincide or are close to the primary points, indicating the absence of chemical changes during heating. A distinct rectilinear section (fit-interval), on the basis of which the B_{anc} estimation was made, is also observed; its associated parameters were calculated (Fig. 2). The vast majority of the obtained B_{anc} definitions meet the necessary criteria of reliability [11]. These estimates, in particular, confirm the results of experiments using the Wilson–Burakov method. The corresponding plots demonstrate the similarity of the NRM and TRM* curves (Fig. 2), and the resulting values of B_{anc}^* are close to the estimates of B_{anc} by the Thellier–Coe method.

Therefore, it was possible to substantiate and confirm comprehensively 38 determinations of B_{anc} obtained by the Thellier–Coe method, which were used in further analysis. At least eight determinations are involved in the calculation of the average B_{anc} value at the sampling site (Table 1). The standard formula [12] was used to calculate VDM:

$$\text{VDM} = 0.5B_{anc}r^3\sqrt{1 + 3\cos^2 I} \times 10^7,$$

where B_{anc} —the average paleointensity at the sampling site, r —the radius of the Earth, and I —the paleomagnetic inclination (the value of 75.6° was used, which was obtained by averaging the entire array of paleomagnetic data on the FJL basalts [9]).

The obtained data indicate that the absolute paleointensity of the geomagnetic field at the Barremian–Aptian boundary was at least four times lower than the current one. The calculated average VDM at the sampling sites, taking into consideration the standard deviation, vary within $(1.3\text{--}2.2) \times 10^{22} \text{ Am}^2$ (Table 1). These anomalously low values of the paleointensity confirm the estimates of the VDM for the $\sim 125 \text{ Ma}$ boundary presented earlier in [6]. Accordingly, there are no grounds to deny the reality of episodes of the dramatic drops in absolute magnetic intensity during the epochs of the prevailing noninversion mode of the geomagnetic field. According to the analysis of the data from the global paleointensity

database, single low VDMs occur over the entire interval of the prevailing high field (135–84 Ma) associated with the Cretaceous superchron (Fig. 3). Within the framework of the standard theoretical models, such changes in the absolute value of the geomagnetic field magnitude are random and are explained by ultrashort events not associated with any significant changes in the mode of geodynamo work and in the general thermodynamics of the Earth's inner shells. However, the available data set allows us to distinguish at least two rather long intervals $\sim 127\text{--}122$ and $108\text{--}104 \text{ Ma}$ in the time of C34n, when the values of the usually high VDM are absent and the average values decrease to $\sim 2 \times 10^{22} \text{ Am}^2$. The third distinct minimum occurs at $\sim 135 \text{ Ma}$ and completes the Jurassic–Early Cretaceous epoch of the low geomagnetic field (Fig. 3).

Analysis of the available data on the age of plume occurrences [14] gives reason to compare quite confidently the indicated episodes of the drop in the paleointensity with the peaks of plume magmatism. Thus, according to numerous U–Pb and $^{40}\text{Ar}/^{39}\text{Ar}$ determinations, the main volume of traps in the Paraná–Etendeka province were formed in the interval 135–132 Ma [14]. One of the largest maximums of plume magmatism in the Earth's history occurred at $\sim 125 \text{ Ma}$ [4, 15–17]. In particular, trap complexes of this age are widely represented as part of the Ontong–Java Province (Manihiki Plateau $\sim 127\text{--}126 \text{ Ma}$). The second outbreak of magmatism within the same province, according to geochronological estimates, occurred at $\sim 95 \text{ Ma}$ (Hikurangi Plateau $\sim 110\text{--}93 \text{ Ma}$; Ontong–Java Plateau $\sim 96 \text{ Ma}$) [14]. At about the same time, $\sim 128\text{--}90 \text{ Ma}$, the main part of the Kerguelen Province was formed [14]. Finally, the main maximum of HALIP magmatism, according to available estimates, corresponds to $\sim 125\text{--}120 \text{ Ma}$, and the second peak, probably much smaller in volume, corresponds to the interval of $\sim 96\text{--}92 \text{ Ma}$ [9, 18, 19]. The formation of a significant part of the Caribbean large igneous province ($\sim 97\text{--}70 \text{ Ma}$) and the Madagascar province ($\sim 90 \text{ Ma}$) can also be associated with the most recent episode of the paleointensity drop [14].

The concepts about the correlation between the geomagnetic field intensity, the frequency of reversals a number of other global indicators, and the formation

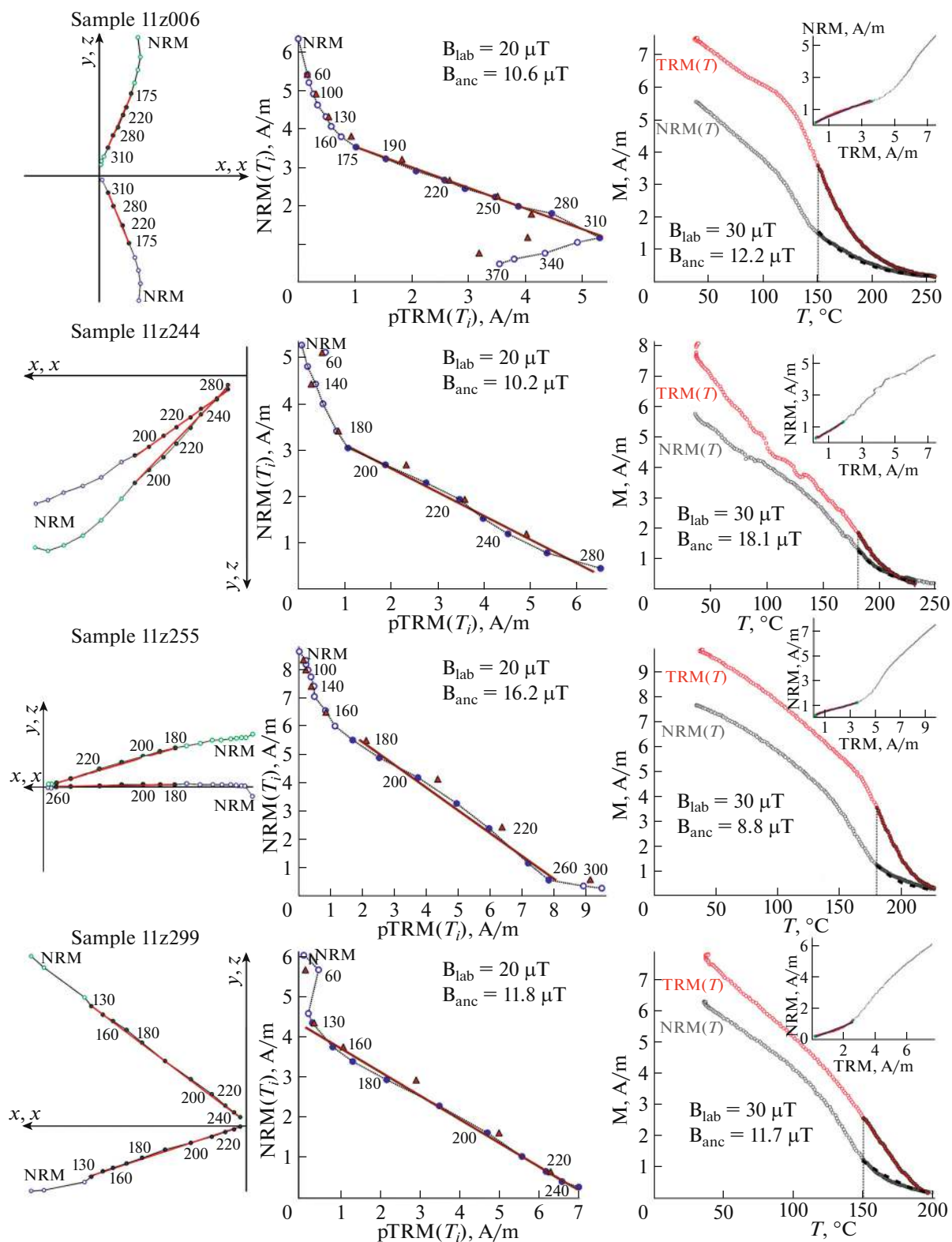


Fig. 2. Typical plots based on the results of paleomagnetic experiments for the Early Cretaceous basalts of the FJL, from left to right: Zijderveld orthogonal diagram (in sample coordinates) based on the results of stepwise thermal demagnetization; Arai-Nagata diagrams for estimation of the absolute paleointensity B_{anc} by the Thellier-Coe method (closed and open points are experimental values included and not included in the approximation interval, red straight line is the trend line, triangles are check points); thermomagnetic curves of NRM, TRM, and TRM^* and the plot of the NRM and TRM dependence for the estimation of paleointensity B_{anc} by the Wilson-Burakov method.

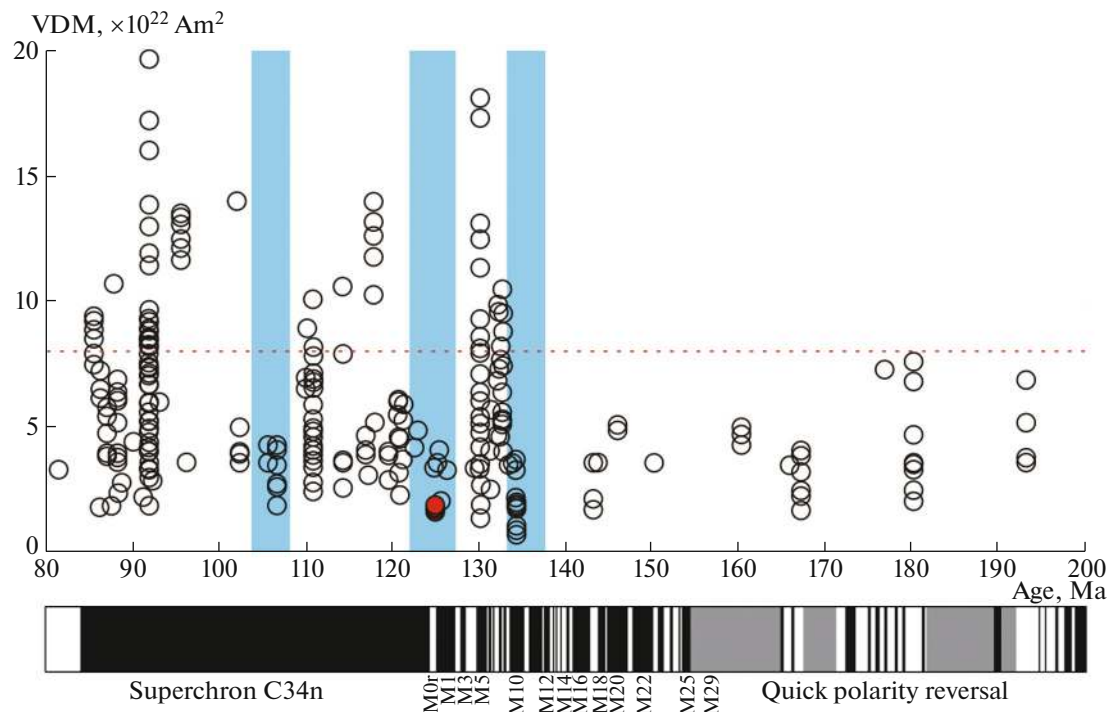


Fig. 3. Comparison of the obtained VDM (red circles) (Table 1) with the available definitions (open circles) for the period 200–80 Ma from [5]. At the bottom, the geomagnetic polarity timescale from [13]; black color corresponds to the intervals of normal polarity, white to reversed polarity, and gray to mixed (frequent reversals out of scale) polarity. The red dashed line shows the present VDM; the blue vertical bars show the intervals of ultra-low VDM.

of mantle plumes are not new [1, 2, 17, 20]. The models explaining this relationship assume the overheating of the outer core due to the fact that conductive transport in the mantle fails to cope with the removal of incoming heat. This leads to a hyperactive mode of the work of the geodynamo, which, among other things, is expressed in an increase in the frequency of reversals. At the same time, the mechanism of polarity reversal itself implies a decrease in intensity during the reversal transition. The entire Jurassic–Early Cretaceous (200–135 Ma) low-field interval can be described by such a state (Fig. 3). Reaching critical temperatures at the core–mantle boundary, as we believe, at 135 Ma, caused the emergence, detachment, and gradual “surfacing” of superheated mantle matter in the form of a plume, which thus removed the excess heat. This almost immediately caused a response to the regime of currents in the outer core and led to a gradual relaxation in the work of the geodynamo. The magnetic field “calmed down,” and the frequency of reversals gradually decreased up to their long-term absence, which corresponded to the superchron. It should be taken into consideration that the magnetic field reacted to heat removal immediately at the origin of the plume, whereas its fixed surface manifestations may have been significantly delayed (up to ~10 million years or more) [2, 20]. This time is necessary for plume ascent and preparation of the cold lithosphere

and sublithosphere source for the active phase of magmatism with the formation of a large igneous province. In this case, the planned episodes of the paleointensity decrease immediately before and during C34n at the levels of ~135, 125, and 105 Ma can be interpreted as a reflection of the final discharge of thermal energy removed from the core and, accordingly, can be correlated with the peaks of plume magmatism during the formation of large igneous provinces, including HALIP.

FUNDING

This study was supported by the Russian Science Foundation, project 23-77-01065 (experiments on the study of paleointensity on the FJL traps and regional analysis of the obtained data) and 24-17-00057 (analysis of the geological structure and geodynamic events in the high-latitude Arctic), and the Ministry of Education and Science of Russia, FSUS-2020-0039 (analysis of the dependence of the geomagnetic field intensity and the evolution of mantle plumes). This research topic is coordinated with the basic research program RAS FWZZ-2022-0001.

CONFLICT OF INTEREST

The authors of this work declare that they have no conflicts of interest.

REFERENCES

1. R. L. Larson and P. Olson, *Earth Planet. Sci. Lett.* **107**, 437–447 (1991).
[https://doi.org/10.1016/0012-821x\(91\)90091-u](https://doi.org/10.1016/0012-821x(91)90091-u)
2. V. Courtillot and P. Olson, *Earth Planet. Sci. Lett.* **260**, 495–504 (2007).
<https://doi.org/10.1016/j.epsl.2007.06.003>
3. A. J. Biggin, B. Steinberger, J. Aubert, et al., *Nat. Geosci.* **5** (8), 526–533 (2012).
<https://doi.org/10.1038/NGEO1521>
4. N. L. Dobretsov, *Russ. Geol. Geophys.* **51** (6), 592–610 (2010).
<https://doi.org/10.1016/j.rgg.2010.05.002>
5. E. V. Kulakov, C. J. Sprain, P. V. Doubrovine, et al., *JGR Solid Earth* **124**, 9999–10022 (2019).
<https://doi.org/10.1029/2018JB017287>
6. A. Di Chiara, L. Tauxe, H. Staudigel, et al., *Geochem., Geophys., Geosyst.* **22** (4), e2020GC009605 (2021).
<https://doi.org/10.1029/2020GC009605>
7. E. M. Bobrovnikova, F. Lhuillier, V. P. Shcherbakov, et al., *JGR Solid Earth* **127**, e2021JB023551 (2022).
<https://doi.org/10.1029/2021JB023551>
8. V. V. Abashev, D. V. Metelkin, N. E. Mikhaltsov, et al., *Russ. Geol. Geophys.* **59** (9), 1161–1181 (2018).
<https://doi.org/10.1016/j.rgg.2018.08.010>
9. D. V. Metelkin, V. V. Abashev, V. A. Vernikovskiy, et al., *Russ. Geol. Geophys.* **63** (4), 342–367 (2022).
<https://doi.org/10.2113/RGG20214432>
10. M. Prévot, E. A. Mankinen, R. S. Coe, and C. S. Grommé, *J. Geophys. Res. B: Solid Earth* **90** (B12), 10417–10448 (1985).
<https://doi.org/10.1029/JB090iB12p10417>
11. V. V. Shcherbakova, V. G. Bakhmutov, D. Thallner, et al., *Geophys. J. Int.* **220** (3), 1928–1946 (2020).
<https://doi.org/10.1093/gji/ggz566>
12. R. T. Merrill, M. W. McElhinny, and P. L. McFadden, *Physics Today* **50** (9), 70 (1997).
<https://doi.org/10.1063/1.881919>
13. J. D. Walker, J. W. Geissman, S. A. Bowring, et al., *GSA Bull.* **125** (3/4), 259–272 (2013).
<https://doi.org/10.1130/B30712.1>
14. Q. Jiang, F. Jourdan, H. K. H. Olierook, and R. E. Merle, *Earth-Sci. Rev.* **237**, 104314 (2023).
<https://doi.org/10.1016/j.earscirev.2023.104314>
15. R. E. Ernst, *Large Igneous Provinces* (Cambridge Univ. Press, Cambridge, 2014).
<https://doi.org/10.15372/GiG2021175>
16. A. N. Didenko and A. I. Khanchuk, *Dokl. Earth Sci.* **487** (2), 873–877 (2019).
<https://doi.org/10.1134/S1028334X19080026>
17. N. L. Dobretsov, D. V. Metelkin, and A. N. Vasilevskiy, *Russ. Geol. Geophys.* **62** (1), 6–24 (2021).
<https://doi.org/10.2113/RGG20204261>
18. V. V. Abashev, D. V. Metelkin, V. A. Vernikovskiy, et al., *Dokl. Earth Sci.* **493** (1), 495–498 (2020).
<https://doi.org/10.1134/S1028334X2007003X>
19. F. Corfu, S. Polteau, S. Planke, et al., *Geol. Mag.* **150** (6), 1127–1135 (2013).
<https://doi.org/10.1017/S0016756813000162>
20. A. N. Didenko, *Russ. Geol. Geophys.* **52** (12), 1530–1538 (2011).
<https://doi.org/10.1016/j.rgg.2011.11.002>

Translated by V. Krutikova

Publisher’s Note. Pleiades Publishing remains neutral with regard to jurisdictional claims in published maps and institutional affiliations.